Journal of The Electrochemical Society

The Electrochemical Society
Advancing solid state & electrochemical science & technology

OPEN ACCESS

Analytical Impedance of PEM Fuel Cell Cathode Including Oxygen Transport in the Channel, Gas Diffusion, and Catalyst Layers

To cite this article: Andrei Kulikovsky 2022 *J. Electrochem. Soc.* **169** 034527

View the article online for updates and enhancements.

The Electrochemical Society
Advancing solid state & electrochemical science & technology
243rd ECS Meeting with SOFC-XVIII
More than 50 symposia are available!
Present your research and accelerate science
Boston, MA • May 28 – June 2, 2023
Learn more and submit!

This content was downloaded from IP address 134.94.122.118 on 02/11/2022 at 05:08

Journal of The Electrochemical Society, 2022 **169** 034527

Analytical Impedance of PEM Fuel Cell Cathode Including Oxygen Transport in the Channel, Gas Diffusion, and Catalyst Layers

Andrei Kulikovsky[1,2,*,z]

[1]*Forschungszentrum Jülich GmbH, Theory and Computation of Energy Materials (IEK–13), Institute of Energy and Climate Research, D–52425 Jülich, Germany*
[2]*Lomonosov Moscow State University, Research Computing Center, 119991 Moscow, Russia*

A model for impedance of a PEM fuel cell cathode taking into account oxygen transport in the cathode catalyst layer (CCL), gas–diffusion layer (GDL) and in channel is solved analytically. A formula for the cathode impedance is valid for the cell current densities below 100 mA cm^{-2} and air flow stoichiometries exceeding 10. Least–squares fitting of experimental spectrum using the analytical result takes about 5 s on a standard PC. Fitting returns Tafel slope of the oxygen reduction reaction, double layer capacitance, CCL proton conductivity and oxygen diffusivities of the CCL and GDL. Analytical impedance can be coded as a user–defined function for a standard spectra fitting software supplied with EIS–meters.

© 2022 The Author(s). Published on behalf of The Electrochemical Society by IOP Publishing Limited. This is an open access article distributed under the terms of the Creative Commons Attribution 4.0 License (CC BY, http://creativecommons.org/licenses/by/4.0/), which permits unrestricted reuse of the work in any medium, provided the original work is properly cited. [DOI: 10.1149/1945-7111/ac5d97]

Manuscript submitted January 16, 2022; revised manuscript received March 8, 2022. Published March 23, 2022.

List of symbols

~	Marks dimensionless variables
b	ORR Tafel slope, V
C_{dl}	Double layer volumetric capacitance, F cm^{-3}
c	Oxygen molar concentration in the CCL, mol cm^{-3}
c_b	Oxygen molar concentration in the GDL, mol cm^{-3}
c_h	Oxygen molar concentration in the channel, mol cm^{-3}
c_h^{in}	Reference (inlet) oxygen concentration, mol cm^{-3}
D_b	Oxygen diffusion coefficient in the GDL, cm^2 s^{-1}
D_{ox}	Oxygen diffusion coefficient in the CCL, cm^2 s^{-1}
F	Faraday constant, C mol^{-1}
f	Characteristic frequency, Hz
h	Cathode channel depth, cm
i_*	ORR volumetric exchange current density, A cm^{-3}
i	Imaginary unit
J	Mean current density in the cell, A cm^{-2}
j	Local proton current density in the CCL, A cm^{-2}
j_0	Local cell current density, A cm^{-2}
l_b	GDL thickness, cm
l_t	CCL thickness, cm
p, q, r, s	Coefficients in equations, Eq. 15
t	Time, s
v	Air flow velocity in the channel, cm s^{-1}
t_*	Characteristic time, s, Eq. 5
x	Coordinate through the cell, cm
Z_{loc}	Local impedance, Ohm cm^2
Z_{tot}	Total cathode side impedance, Ohm cm^2
z	Coordinate along the cathode channel, cm
Subscripts:	
0	Membrane/CCL interface
1	CCL/GDL interface
b	GDL
h	Air channel
Superscripts:	
0	Steady–state value
1	Small–amplitude perturbation
Greek:	
α, β	Dimensionless parameters, Eq. 22

(Continued).

η	ORR overpotential, positive by convention, V
ε	Dimensionless parameter, Eq. 8
λ	Air flow stoichiometry, Eq. 28
μ	Dimensionless parameter, Eq. 8
σ_p	CCL proton conductivity, S cm^{-1}
ξ	Dimensionless parameter, Eq. 28
ω	Angular frequency of the AC signal, s^{-1}

Polymer electrolyte membrane fuel cells (PEMFCs) are pollution–free electrochemical power sources realizing direct conversion of chemical energy of reactants into electric current. At present, PEMFC–based cars are available on the market. However, much work needs to be done to improve reliability and reduce cost of PEMFCs. One of the key problems in the PEMFC technology is development of fast and reliable methods for cell/stack characterization.

Electrochemical impedance spectroscopy (EIS) is a non–invasive tool for in situ measurements of transport and kinetic properties of PEM fuel cell functional layers.[1,2] Impedance spectra can be measured by applying a small–amplitude voltage or current perturbation to the operating fuel cell, without interruption of current production mode. Unlike static methods, EIS allows us to separate contributions of different processes into the total voltage loss in the cell, which makes impedance spectroscopy an extremely powerful and attractive tool for cells design and testing. However, deciphering of impedance spectra requires modeling.

A simplest method of spectra analysis is construction of equivalent circuit (EC) having the impedance spectrum close to the experimental spectrum of interest (see e.g.,[3,4]). Fitting of EC spectrum to the measured one makes it possible to associate EC elements (resistors, capacitors etc.) with the physical processes inside the cell. However, since any selected EC is not unique, this method is unreliable and it may lead to erroneous results (see critics of EC method in Ref. 5). Nonetheless, software for least–squares spectra fitting with a user–defined EC is supplied with modern EIS–meters providing wide usage of this method in labs.

After pioneering numerical impedance model of Springer et al.[6] and analytical work of Eikerling and Kornyshev[7] there has been a growing interest in physics–based impedance modeling (see reviews[8,9]). The models of this type are based on transient charge and mass conservation equations for oxygen reduction reaction (ORR) participants. Of particular interest are analytical models, as

*Electrochemical Society Member.
[z]E-mail: A.Kulikovsky@fz-juelich.de

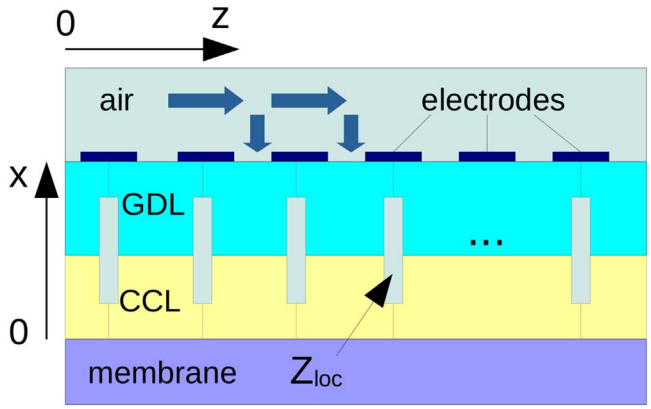

Figure 1. Schematic of a PEM fuel cell cathode with the straight channel and segmented electrodes. CCL and GDL stand for cathode catalyst layer and gas diffusion layer, respectively.

they improve our understanding of the nature of impedance components inside the cell.

Below, analytical model for the PEMFC cathode side impedance is developed. The model includes oxygen transport in the channel, gas diffusion layer (GDL), and in the cathode catalyst layer (CCL), as well as proton transport in the CCL and ORR. Over the past decade, partial models for impedance of one or two components from the list above have been developed, e.g., a model for CCL impedance[10] constructed under assumption of fast oxygen transport in the GDL and channel, a model for CCL+GDL impedance[11] assuming fast oxygen transport in the channel, and a model for GDL +channel impedance,[12] which ignores oxygen and proton transport losses in the CCL. A lot of efforts have been done to develop a numerical model suitable for fitting impedance spectra measured for cell currents up to 1 A cm^{-2}, which are of large practical interest. The numerical model is described in Refs. 13, 14 and summarized in Ref. 15. The numerical model takes into account oxygen transport in the channel, GDL and CCL, and it is suitable for fitting high–current spectra. However, the cost of numerical nature of this model is rather high: fitting either required a parallel computer with the number of cores on the order of hundred, or it takes quite a lot of time, typically about one hour. There is a need in "reference" analytical model for fast spectra fitting.

Recently, it has been shown that the oxygen transport processes in the cell are interdependent, and hence it is important to incorporate all of them into a single model.[16] Below, all the aforementioned processes are taken into account and analytical formula for the cathode side impedance is derived. Fitting of real spectra using this formula returns transport parameters of the cell functional layers. The obtained impedance can be coded as a user–defined function for the standard spectra fitting software supplied with EIS–meters.

Transport Equations in Catalyst Layer

The cathode side of a PEM fuel cell considered in this work is shown schematically in Fig. 1. Oxygen transported with the air flow along the straight cathode channel diffuses through the gas diffusion layer (GDL) to the cathode catalyst layer (CCL), where the ORR occurs.

The impedance model below is derived from the transient charge and mass conservation equations in the channel, GDL and CCL. The core of the model is a transient model for the CCL performance. Porous CCL is considered as unstructured macro–homogeneous media with effective transport parameters for oxygen, protons and electrons. As the CCL electron conductivity is usually much larger than the proton conductivity, the CCL performance is described by three equations[17]

$$C_{dl}\frac{\partial\eta}{\partial t}+\frac{\partial j}{\partial x}=-i_*\left(\frac{c}{c_h^{in}}\right)\exp\left(\frac{\eta}{b}\right) \quad [1]$$

$$j=-\sigma_p\frac{\partial\eta}{\partial x} \quad [2]$$

$$\frac{\partial c}{\partial t}-D_{ox}\frac{\partial^2 c}{\partial x^2}=-\frac{i_*}{4F}\left(\frac{c}{c_h^{in}}\right)\exp\left(\frac{\eta}{b}\right). \quad [3]$$

Here t is time, x is the coordinate through the cell counted from the membrane surface (Fig. 1), C_{dl} is the volumetric double layer capacitance (F cm^{-3}), η is the positive by convention ORR overpotential, j is the local proton current density in the CCL, i_* is the ORR exchange current density, c is the local oxygen concentration in the CCL, c_h^{in} is the reference (inlet) oxygen concentration, b is the ORR Tafel slope, σ_p is the CCL proton conductivity, D_{ox} is the effective oxygen diffusion coefficient in the CCL, and F is the Faraday constant. Equation 1 is the proton charge conservation equation, which includes displacement current (the first term on the left side) and the Tafel rate of proton current consumption in the ORR (the right side). Equation 2 is the Ohm's law, and Eq. 3 is the oxygen diffusion equation with the sink term on the right side due to oxygen consumption in the ORR.

It is convenient to introduce dimensionless variables

$$\tilde{t}=\frac{t}{t_*},\quad \tilde{x}=\frac{x}{l_t},\quad \tilde{c}=\frac{c}{c_h^{in}},\quad \tilde{\eta}=\frac{\eta}{b},\quad \tilde{j}=\frac{j}{j_*},$$
$$\tilde{D}=\frac{4FDc_h^{in}}{\sigma_p b},\quad \tilde{\omega}=\omega t_*,\quad \tilde{Z}=\frac{Z\sigma_p}{l_t}, \quad [4]$$

where

$$t_*=\frac{C_{dl}b}{i_*},\quad j_*=\frac{\sigma_p b}{l_t}, \quad [5]$$

ω is the angular frequency of applied signal and Z is the impedance. Substituting Eq. 2 into Eq. 1 and using the dimensionless variables 4 we come to the system of two equations for $\tilde{\eta}$ and $\tilde{c}$

$$\frac{\partial\tilde{\eta}}{\partial\tilde{t}}-\varepsilon^2\frac{\partial^2\tilde{\eta}}{\partial\tilde{x}^2}=-\tilde{c}\exp\tilde{\eta},\quad \tilde{\eta}(0)=\tilde{\eta}^0,\ \frac{\partial\tilde{\eta}}{\partial\tilde{x}}\bigg|_{\tilde{x}=1}=0, \quad [6]$$

$$\mu^2\frac{\partial\tilde{c}}{\partial\tilde{t}}-\varepsilon^2\tilde{D}_{ox}\frac{\partial^2\tilde{c}}{\partial\tilde{x}^2}=-\tilde{c}\exp\tilde{\eta},\quad \frac{\partial\tilde{c}}{\partial\tilde{x}}\bigg|_{\tilde{x}=0}=0,\ \tilde{c}(1)=\tilde{c}_1, \quad [7]$$

where the dimensionless parameters μ and ε are given by

$$\mu=\sqrt{\frac{4Fc_h^{in}}{C_{dl}b}},\quad \varepsilon=\sqrt{\frac{\sigma_p b}{i_* l_t^2}}. \quad [8]$$

A standard procedure of linearization and Fourier transform includes substitution of small–amplitude harmonic perturbations of the form

$$\tilde{c}(\tilde{x},\tilde{t})=\tilde{c}^0(\tilde{x})+\tilde{c}^1(\tilde{x},\tilde{\omega})\exp(i\tilde{\omega}\tilde{t}),\quad \tilde{c}^1\ll\tilde{c}^0$$
$$\tilde{\eta}(\tilde{x},\tilde{t})=\tilde{\eta}^0(\tilde{x})+\tilde{\eta}^1(\tilde{x},\tilde{\omega})\exp(i\tilde{\omega}\tilde{t}),\quad \tilde{\eta}^1\ll\tilde{\eta}^0 \quad [9]$$

to Eqs. 6, 7, subtraction of static equations, Taylor series expansion of exponent, and neglect of the term with perturbations product.[15] Here, the superscripts 0 and 1 mark the static and perturbed variables. This procedure leads to a system of linear equations for the perturbation amplitudes $\tilde{\eta}^1$ and $\tilde{c}^1$

$$\varepsilon^2\frac{\partial^2\tilde{\eta}^1}{\partial\tilde{x}^2} = e^{\tilde{\eta}^0}\tilde{c}^1 + (\tilde{c}^0 e^{\tilde{\eta}^0} + i\tilde{\omega})\tilde{\eta}^1,$$
$$\tilde{\eta}^1(1) = \tilde{\eta}_1^1, \quad \left.\frac{\partial\tilde{\eta}^1}{\partial\tilde{x}}\right|_{\tilde{x}=1} = 0, \qquad [10]$$

$$\varepsilon^2\tilde{D}_{ox}\frac{\partial^2\tilde{c}^1}{\partial\tilde{x}^2} = (e^{\tilde{\eta}^0} + i\tilde{\omega}\mu^2)\tilde{c}^1 + \tilde{c}^0 e^{\tilde{\eta}^0}\tilde{\eta}^1$$
$$\left.\frac{\partial\tilde{c}^1}{\partial\tilde{x}}\right|_{\tilde{x}=0} = 0, \quad \tilde{c}^1(1) = \tilde{c}_1^1. \qquad [11]$$

where $\tilde{\eta}_1^1$ is the applied potential perturbation and $\tilde{c}_1^1$ is the oxygen concentration perturbation at the CCL/GDL interface (at $\tilde{x} = 1$). Solution of Eqs. 10, 11 allows us to calculate system impedance $\tilde{Z}$

$$\tilde{Z} = -\left.\frac{\tilde{\eta}^1}{\partial\tilde{\eta}^1/\partial\tilde{x}}\right|_{\tilde{x}=0}. \qquad [12]$$

Note that the contribution of GDL and channel impedance is described by the term $\tilde{c}_1^1$ in the right boundary condition for Eq. 11. In other words, the term $\tilde{c}_1^1$ plays a role of "interface" to the GDL and channel impedance in the system.

Dividing Eq. 10 by ε^2 and Eq. 11 by $\varepsilon^2\tilde{D}_{ox}$ we get a boundary-–value problem of the form

$$\frac{\partial^2\tilde{\eta}^1}{\partial\tilde{x}^2} = p\tilde{c}^1 + q\tilde{\eta}^1, \quad \tilde{\eta}^1(1) = \tilde{\eta}_1^1, \quad \left.\frac{\partial\tilde{\eta}^1}{\partial\tilde{x}}\right|_{\tilde{x}=1} = 0, \qquad [13]$$

$$\frac{\partial^2\tilde{c}^1}{\partial\tilde{x}^2} = r\tilde{c}^1 + s\tilde{\eta}^1, \quad \left.\frac{\partial\tilde{c}^1}{\partial\tilde{x}}\right|_{\tilde{x}=0} = 0, \quad \tilde{c}^1(1) = \tilde{c}_1^1, \qquad [14]$$

where p, q, r, s are given by

$$p = \frac{e^{\tilde{\eta}^0}}{\varepsilon^2}, \quad q = \frac{\tilde{c}^0 e^{\tilde{\eta}^0} + i\tilde{\omega}}{\varepsilon^2},$$
$$r = \frac{e^{\tilde{\eta}^0} + i\tilde{\omega}\mu^2}{\varepsilon^2\tilde{D}_{ox}}, \quad s = \frac{\tilde{c}^0 e^{\tilde{\eta}^0}}{\varepsilon^2\tilde{D}_{ox}}. \qquad [15]$$

Impedance

CCL impedance.—In general, the coefficients p, q, r, s in Eqs. 13, 14 are functions of coordinate, which makes analytical solution of this system hardly possible. However, if the cell current density is sufficiently small (see below), the static shapes of the oxygen concentration $\tilde{c}^0$ and overpotential $\tilde{\eta}^0$ are nearly independent of $\tilde{x}$ and the system 14, 13 can be solved. Solution of the system with constant coefficients could be derived using either a classic method of constructing characteristic polynomial, or a math software (e.g., Maple® or Mathematica®). In either case the resulting functions $\tilde{c}^1(\tilde{x})$ and $\tilde{\eta}^1(\tilde{x})$ are extremely cumbersome and are not displayed here.

Fortunately, calculation of the system impedance from Eq. 12 leads to a reasonably compact result

$$\tilde{Z} = \frac{A_1\tilde{\eta}_1^1 + A_2\tilde{c}_1^1}{B_1\tilde{\eta}_1^1 + B_2\tilde{c}_1^1} \qquad [16]$$

where the coefficients A_1, A_2, B_1, B_2 are given by Eqs. A·1–A·4 (Appendix).

As noted above, oxygen concentration perturbation $\tilde{c}_1^1$ in Eq. 16 provides interface to the GDL and channel impedance. In the simplest case, one may set $\tilde{c}_1^1 = 0$, meaning that the oxygen transport in the GDL and channel is assumed to be fast and the respective impedances are ignored. Solution of Eqs. 10, 11 then gives a "pure" CCL impedance[10]

$$\tilde{Z}_{ccl} = \frac{A_1}{B_1}. \qquad [17]$$

For further references we note that solution of the system 13, 14 gives the following result for the flux $D_{ox}\partial\tilde{c}^1/\partial\tilde{x}|_{\tilde{x}=1}$

$$D_{ox}\left.\frac{\partial\tilde{c}^1}{\partial\tilde{x}}\right|_{\tilde{x}=1} = \frac{A_\eta\tilde{\eta}_1^1 + A_c\tilde{c}_1^1}{B_N}, \qquad [18]$$

where A_η, A_c and B_N are given by Eqs. A·6–A·8 (Appendix).

CCL + GDL impedance.—To take into account impedance of oxygen transport in the GDL, we write diffusion equation for the oxygen concentration c_b in the GDL

$$\frac{\partial c_b}{\partial t} - D_b\frac{\partial^2 c_b}{\partial x^2} = 0 \qquad [19]$$

where D_b is the GDL oxygen diffusivity. Equation 19 is linear and hence equation for the oxygen concentration perturbation $\tilde{c}_b^1$ is

$$\varepsilon^2\tilde{D}_b\frac{\partial^2\tilde{c}_b^1}{\partial\tilde{x}^2} = i\tilde{\omega}\mu^2\tilde{c}_b^1, \quad \tilde{D}_b\left.\frac{\partial\tilde{c}_b^1}{\partial\tilde{x}}\right|_{\tilde{x}=1} = \tilde{D}_{ox}\left.\frac{\partial\tilde{c}^1}{\partial\tilde{x}}\right|_{\tilde{x}=1},$$
$$\tilde{c}_b^1(1 + \tilde{l}_b) = \tilde{c}_h^1, \qquad [20]$$

where the left boundary condition means continuity of oxygen flux at the CCL/GDL interface, and the right boundary condition expresses continuity of oxygen concentration at the GDL/channel interface. Solution to Eq. 20 leads to the following relation for $\tilde{c}_1^1 = \tilde{c}_b^1$ (Ref. 13):

$$\tilde{c}_1^1 = -\alpha\tilde{D}_{ox}\left.\frac{\partial\tilde{c}^1}{\partial\tilde{x}}\right|_{\tilde{x}=1} + \beta\tilde{c}_h^1 \qquad [21]$$

where

$$\alpha = \frac{\tanh\left(\mu\tilde{l}_b\sqrt{i\tilde{\omega}/(\varepsilon^2\tilde{D}_b)}\right)}{\mu\sqrt{i\tilde{\omega}\tilde{D}_b/\varepsilon^2}},$$
$$\beta = \frac{1}{\cosh\left(\mu\tilde{l}_b\sqrt{i\tilde{\omega}/(\varepsilon^2\tilde{D}_b)}\right)} \qquad [22]$$

and l_b is the GDL thickness.

Substituting Eq. 18 into Eq. 21 and solving the resulting equation for $\tilde{c}_1^1$, we get

$$\tilde{c}_1^1 = \frac{-\alpha A_\eta\tilde{\eta}_1^1 + \beta B_N\tilde{c}_h^1}{\alpha A_c + B_N} \qquad [23]$$

With this $\tilde{c}_1^1$, Eq. 16 transforms to

$$\tilde{Z} = \frac{(\alpha(A_1A_c - A_2A_\eta) + A_1B_N)\tilde{\eta}_1^1 + \beta A_2B_N\tilde{c}_h^1}{(\alpha(A_cB_1 - A_\eta B_2) + B_1B_N)\tilde{\eta}_1^1 + \beta B_2B_N\tilde{c}_h^1}. \qquad [24]$$

Equation 24 contains "interface" to the channel impedance through the term with $\tilde{c}_h^1$. Setting in Eq. 24 $\tilde{c}_h^1 = 0$, we get the CCL + GDL impedance of the cell under infinite stoichiometry of the oxygen (air) flow corresponding to zero channel impedance:

$$\tilde{Z}_{ccl+gdl} = \frac{\alpha(A_1A_c - A_2A_\eta) + A_1B_N}{\alpha(A_cB_1 - A_\eta B_2) + B_1B_N}. \quad \lambda \to \infty \qquad [25]$$

It is easy to verify that in the limit of $\tilde{D}_b \to \infty$ (zero GDL impedance), we have $\alpha \to 0$ and Eq. 25 reduces to Eq. 17.

CCL + GDL + channel impedance.—The simplest approximation for oxygen transport in the channel provides plug flow equation

$$\frac{\partial c_h}{\partial t} + v\frac{\partial c_h}{\partial z} = -\frac{D_b}{h}\frac{\partial c_b}{\partial x}\bigg|_{x=l_t+l_b}, \qquad [26]$$

where c_h is the oxygen concentration in channel, z is the coordinate along the channel, v is the constant air flow velocity, and the right side represents the diffusive oxygen flux in the GDL at the channel/GDL interface. Equation 26 describes in a 1d+1d manner oxygen "leakage" to the GDL while the flow moves along the cathode channel.

Equation 26 leads to equation for the dimensionless perturbation of oxygen concentration $\tilde{c}_h^1$ (Ref. 12):

$$\lambda\tilde{J}\frac{\partial\tilde{c}_h^1}{\partial\tilde{z}} = -\mathrm{i}\tilde{\omega}\xi^2\tilde{c}_h^1 - \tilde{D}_b\frac{\partial\tilde{c}_b^1}{\partial\tilde{x}}\bigg|_{\tilde{x}=1+\tilde{l}_b}, \qquad [27]$$

where ξ is the dimensionless parameter, and λ is the stoichiometry of air flow:

$$\xi = \sqrt{\frac{4Fhc_h^{in}l_t i_*}{C_{dl}\sigma_p b^2}}, \quad \lambda = \frac{4Fhvc_h^{in}}{LJ}. \qquad [28]$$

Calculation of the flux $\tilde{D}_b\partial\tilde{c}_b^1/\partial\tilde{x}|_{\tilde{x}=1+\tilde{l}_b}$ from solution of Eq. 20 results in

$$\tilde{D}_b\frac{\partial\tilde{c}_b^1}{\partial\tilde{x}}\bigg|_{\tilde{x}=1+\tilde{l}_b} = \left(\frac{\alpha\mu^2\tilde{D}_b}{\varepsilon^2}\right)\mathrm{i}\tilde{\omega}\tilde{c}_h^1 + \beta D_{ox}\frac{\partial\tilde{c}^1}{\partial\tilde{x}}\bigg|_{\tilde{x}=1}. \qquad [29]$$

Taking into account Eqs. 29 and 18, Eq. 27 transforms to

$$\lambda\tilde{J}\frac{\partial\tilde{c}_h^1}{\partial\tilde{z}} = -\left(\mathrm{i}\tilde{\omega}\left(\xi^2 + \frac{\alpha\mu^2\tilde{D}_b}{\varepsilon^2}\right) + \frac{\beta^2A_c}{\alpha A_c + B_N}\right)\tilde{c}_h^1 - \frac{\beta A_\eta\tilde{\eta}_1^1}{\alpha A_c + B_N}. \qquad [30]$$

It is convenient to denote coefficients on the right side of Eq. 30 as Q and P, which leads us to the problem

$$\lambda\tilde{J}\frac{\partial\tilde{c}_h^1}{\partial\tilde{z}} = -Q\tilde{c}_h^1 - P\tilde{\eta}_1^1, \quad \tilde{c}_h^1(0) = 0 \qquad [31]$$

where

$$Q = \mathrm{i}\tilde{\omega}\left(\xi^2 + \frac{\alpha\mu^2\tilde{D}_b}{\varepsilon^2}\right) + \frac{\beta^2A_c}{\alpha A_c + B_N}, \quad P = \frac{\beta A_\eta}{\alpha A_c + B_N}. \qquad [32]$$

In general, the static shape of oxygen concentration $\tilde{c}^0$ depends on coordinate along the channel $\tilde{z}$, meaning that P and Q depend on $\tilde{z}$. However, when the oxygen (air) stoichiometry is sufficiently large, this dependence is weak and it can be neglected. In this case solution to Eq. 31 is

$$\tilde{c}_h^1(\tilde{z}) = \frac{P}{Q}\left(\exp\left(-\frac{Q\tilde{z}}{\lambda\tilde{J}}\right) - 1\right)\tilde{\eta}_1^1, \quad \lambda \gg 1. \qquad [33]$$

Using Eq. 33 in 24, we find the general formula for local impedance of the PEMFC cathode side at a distance $\tilde{z}$ from the channel inlet:

$$\tilde{Z}_{loc}(\tilde{z}) = \frac{\alpha(A_1A_c - A_2A_\eta) + A_1B_N + \beta A_2B_NP(\exp(-Q\tilde{z}/(\lambda\tilde{J})) - 1)/Q}{\alpha(A_cB_1 - A_\eta B_2) + B_1B_N + \beta B_2B_NP(\exp(-Q\tilde{z}/(\lambda\tilde{J})) - 1)/Q} \qquad [34]$$

Equation 34 can be used for processing of local impedance spectra measured in the cell with segmented electrodes. Note that Eq. 33 works if variation of all transport parameters along the channel is weak.

As local impedances are connected in parallel (Fig. 1), total cathode impedance $\tilde{Z}_{tot}$ is given by

$$\tilde{Z}_{tot} = \left(\int_0^1 \frac{d\tilde{z}}{\tilde{Z}_{loc}}\right)^{-1}. \qquad [35]$$

Denoting

$$X_1 = \alpha(A_1A_c - A_2A_\eta) + A_1B_N, \quad Y_1 = \beta A_2B_NP/Q,$$
$$X_2 = \alpha(A_cB_1 - A_\eta B_2) + B_1B_N, \quad Y_2 = \beta B_2B_NP/Q,$$
$$R = Q/(\lambda\tilde{J}), \qquad [36]$$

Equation 34 takes the form

$$\tilde{Z}_{loc} = \frac{X_1 + Y_1(\exp(-R\tilde{z}) - 1)}{X_2 + Y_2(\exp(-R\tilde{z}) - 1)}. \qquad [37]$$

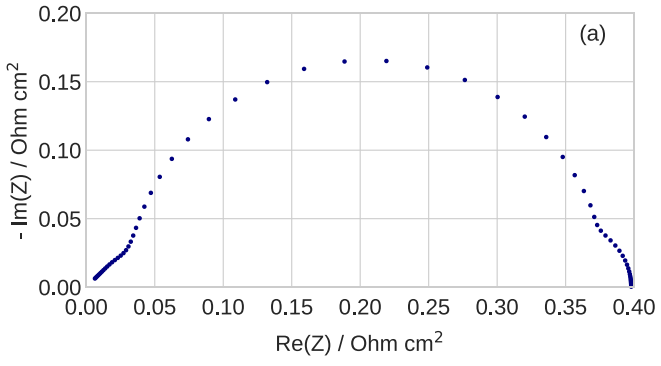

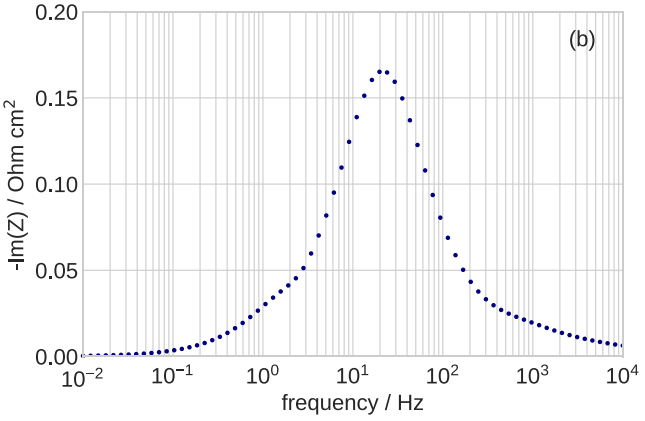

Figure 2. (a) Example of the Nyquist spectrum of Eq. 38. Parameters for calculations are listed in Table I. (b) Frequency dependence of imaginary part of the spectrum in (a).

Table I. The cell parameters used in calculations.

CCL thickness l_t, cm	$10 \cdot 10^{-4}$
GDL thickness l_b, cm	$230 \cdot 10^{-4}$
CCL oxygen diffusivity D_{ox}, cm^2 s^{-1}	$1 \cdot 10^{-4}$
GDL oxygen diffusivity D_b, cm^2 s^{-1}	0.02
CCL proton conductivity σ_p S cm^{-1}	0.01
ORR Tafel slope b, mV / exp	30
Double layer capacitance C_{dl}, F cm^{-3}	20
Air channel depth h, cm	0.1
Air flow stoichiometry λ	9.5
Cell current density j_0, A cm^{-2}	0.1
Pressure	Standard
Cell temperature T, K	273 + 80

Calculating integral 35, we finally find

$$\tilde{Z}_{tot} = \frac{(Y_1 - X_1)R}{\left(X_1\frac{Y_2}{Y_1} - X_2\right)\ln\left(1 + \frac{Y_1}{X_1}(\exp(-R) - 1)\right) + (Y_2 - X_2)R}. \quad [38]$$

Equation 38 is the general analytical result for the total cathode side impedance of a PEM fuel cell. This equation takes into account oxygen transport in the channel, GDL, CCL, proton transport in the CCL and faradaic reaction. Equation 38 is fast for numerical calculations of impedance and hence it is most suitable for nonlinear least–squares fitting of experimental spectra, as discussed below.

Limits of validity.—The calculations above have been done assuming that the static oxygen concentration in the CCL $\bar{c}^0$ and overpotential $\bar{\eta}^0$ are nearly independent of $\bar{x}$. This assumption is fulfilled if the mean cell current density J is sufficiently small:

$$J \ll \min\left\{j_p = \frac{\sigma_p b}{l_t}, \quad j_{ox} = \frac{4FD_{ox}c_h^{in}}{l_t}\right\} \quad [39]$$

where j_p and j_{ox} are the characteristic current densities of the proton and oxygen transport in the CCL.[18] For typical PEMFC parameters, Eq. 39 holds for the cell current densities below 100 mA cm^{-2}. Further, assumption of small variation of the static oxygen concentration along the channel, which was used to integrate Eq. 31 holds if this variation is less than 10%. This means that Eq. 38 is valid provided that the air flow stoichiometry $\lambda \gtrsim 10$.

Numerical Results and Discussion

Figure 2a shows the Nyquist spectrum of Eq. 38 for the cell parameters listed in Table I. Figure 2b depicts the frequency dependence of imaginary part of impedance Eq. 38. The spectrum consists of two arcs, of which the small low–frequency (LF) one is due to oxygen transport in the channel. The large medium–frequency (MF) arc includes oxygen transport in the GDL and CCL, and faradaic impedance. The high–frequency (HF) straight line in Fig. 2a

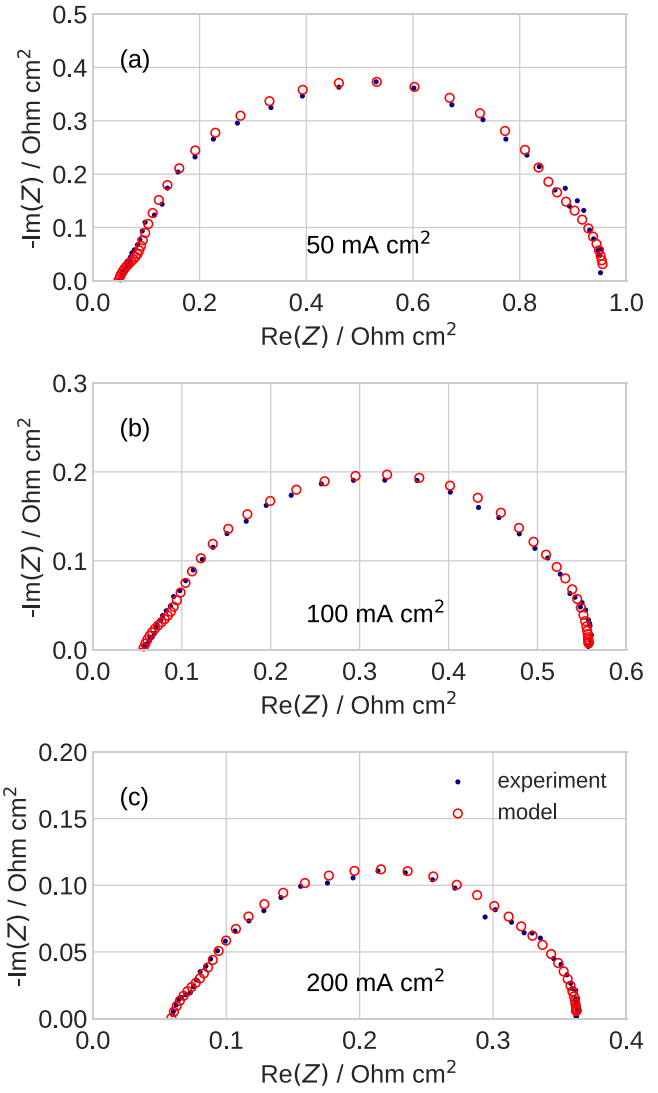

Figure 3. Experimental (solid points) and fitted Eq. 38 (open circles) Nyquist spectra of a standard PEM fuel cell for the current density of (a) 50 mA cm^{-2}, (b) 100 mA cm^{-2}, and (c) 200 mA cm^{-2}.

Table II. The fitting parameters (upper part) and cell operating conditions (lower part). The ORR Tafel slope is given in mV/exp; to obtain the values in mV/decade the numbers in Table should be multiplied by 2.3.

Current density, mA cm^{-2}	50	100	200
ORR Tafel slope b, mV / exp	32.6 ± 0.3	33.6 ± 0.4	38.0 ± 0.4
CCL proton conductivity σ_p / mS cm^{-1}	6.3 ± 0.5	7.4 ± 0.5	9.1 ± 0.6
Double layer capacitance C_{dl} / F cm^{-3}	24.3 ± 0.4	22.6 ± 0.5	17.9 ± 0.5
CCL oxygen diffusivity $D_{ox}/10^{-4}$ / cm^2 s^{-1}	0.25 ± 0.06	0.4 ± 0.1	0.9 ± 0.1
GDL oxygen diffusivity D_b / cm^2 s^{-1}	—	—	0.013 ± 0.004
HF resistance R_{HFR} / mOhm cm^2	28 ± 3	39 ± 2	42 ± 1
Cable inductance $L_{cab}/10^{-9}$, Henry	30 ± 7	22 ± 3	17 ± 2
Air flow stoichiometry λ		9.5	
Pressure, bar		1.5	
Air flow relative humidity RH, %		50	
Cell temperature T, K		273 + 80	

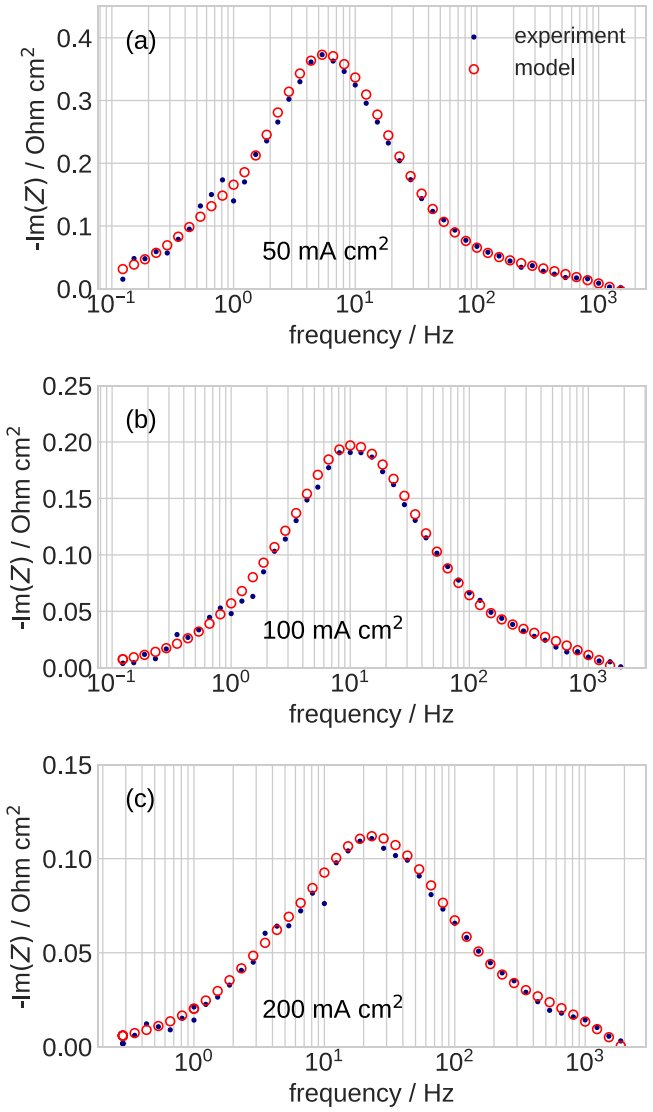

Figure 4. Experimental (solid points) and fitted Eq. 38 (open circles) frequency dependencies of imaginary part of impedance in Fig. 3.

exhibits proton transport impedance.[7] Calculation of the spectra in Fig. 2 with 72 points (12 points per decade) using Python code takes less than 0.01 sec on a standard 2.4 GHz PC.

Of particular interest is application of Eq. 38 for fitting experimental impedance spectra. As an example, three spectra of a standard PEM fuel cell operated at the current densities of 50, 100 and 200 mA cm^{-2} have been fitted. The main experimental conditions are listed in the bottom part of Table II; detailed description of experimental conditions and procedure of EIS measurements can be found in Ref. 14. Fitting has been performed using a least–squares procedure *least_squares* with the *"trf"* method from the Python library SciPy. Fitting of a single spectrum using a custom parallel code takes about 5 s on a PC equipped with a quad–core processor. To better describe the HF part of the spectra, inductive cable impedance $Z_{cab} = i\omega L_{cab} S_{cell}$ has been added in series with Z_{tot}, Eq. 38. Here, L_{cab} is the cable inductance and $S_{cell} = 76$ cm^2 is the active cell surface area. Figure 3 shows measured and fitted spectra; the fitting parameters and the estimates of their accuracy are collected in the upper part of Table II.

At low currents of 50 and 100 mA cm^{-2} the contribution of GDL impedance to the total impedance is small and parameter D_b has not been measured accurately (Table II). However, at 200 mA cm^{-2} fitting returns quite a reasonable value of $D_b \simeq 0.013$ cm^2 s^{-1} (Table II). Though the current density exceeds the limit given by Eq. 39, Figs. 3c, 4c and Table II show that the model still can be used, at least to estimate the transport parameters. The other parameters agree well with the literature data and with our previous publications (see details and references in Ref. 15). Note the linear growth of D_{ox} with the cell current density (Table II). The origin of this growth yet is unknown. Note also that impedance spectrum measured at a constant cell current provides an instant "shoot" of the cell state. Liquid water saturation s effects are taken into account implicitly, through the values of transport parameters in the model equations. In other words, the values of σ_p, D_{ox} and D_b depend implicitly on s.

Recently, it has been shown that impedance of two oxygen transport layers cannot be represented as a sum of separate layer impedances.[16] Every layer "feels" impedance of the neighboring layer, so that the two–layer system works as a unified oxygen transport media. This result means that impedances of all oxygen transport medias in a PEMFC (channel, GDL, CCL, and, perhaps, ionomer film covering Pt/C agglomerates in the CCL) are interdependent. In other words, impedance models ignoring impedance of any transport element in the list above are, strictly speaking, not accurate. The model above is a first one incorporating virtually all oxygen transport medias in a standard PEMFC, where the effect of ionomer film is negligible.

Conclusions

A model for PEM fuel cell impedance including oxygen transport in the channel, gas–diffusion and catalyst layers is developed. Analytical solution for the cathode side impedance which takes into account aforementioned oxygen transport processes and proton transport in the CCL is derived. The solution is valid for cell current densities below 100 mA cm^{-2} and air flow stoichiometry above 10. Fitting of experimental impedance spectra using the analytical formula takes about 5 s on a standard quad–core PC. Fitting returns oxygen transport parameters in the functional layers, proton conductivity of the CCL, ORR Tafel slope and double layer capacitance. The derived formula for impedance can be coded as a user–defined function for the standard software for spectra fitting supplied with EIS–meters.

Appendix: Coefficients in Equations

The coefficients in Eq. 16 are given by

$$A_1 = 4\phi_1\phi_2(2ps + (q-r)^2)\cosh\left(\frac{\phi_1}{2}\right)\cosh\left(\frac{\phi_2}{2}\right) + 8ps\left(2(q+r)\sinh\left(\frac{\phi_1}{2}\right)\sinh\left(\frac{\phi_2}{2}\right) + \phi_1\phi_2\right) \quad [A\cdot1]$$

$$A_2 = 4p(q-r)\phi_1\phi_2\cosh\left(\frac{\phi_1}{2}\right)\cosh\left(\frac{\phi_2}{2}\right) + 4p\left(4(2ps - r(q-r))\sinh\left(\frac{\phi_1}{2}\right) \times \sinh\left(\frac{\phi_2}{2}\right) - (q-r)\phi_1\phi_2\right) \quad [A\cdot2]$$

$$B_1 = \phi_1\cosh\left(\frac{\phi_1}{2}\right)\sinh\left(\frac{\phi_2}{2}\right) \times ((2ps + (q-r)(q-r-\psi)\phi_2^2 + 4ps(q+r-\psi)) + \phi_2\sinh\left(\frac{\phi_1}{2}\right)\cosh\left(\frac{\phi_2}{2}\right) \times ((2ps + (q-r)(q-r+\psi))\phi_1^2 + 4ps(\psi+q+r)) \quad [A\cdot3]$$

$$B_2 = \phi_1 \cosh\left(\frac{\phi_1}{2}\right)\sinh\left(\frac{\phi_2}{2}\right)(p(q - r - \psi)\phi_2^2 + 4p(2ps - r(q - r + \psi))) + \phi_2 \sinh\left(\frac{\phi_1}{2}\right)\cosh\left(\frac{\phi_2}{2}\right) \times (p(q - r + \psi)\phi_1^2 + 4p(2ps - r(q - r - \psi))) \quad [A\cdot4]$$

$$\phi_1 = \sqrt{2(q + r) + 2\psi}$$
$$\phi_2 = \sqrt{2(q + r) - 2\psi}$$
$$\psi = \sqrt{4ps + (q - r)^2} \quad [A\cdot5]$$

The coefficients in Eq. 18 are

$$A_\eta = s\tilde{D}_{ox}(\phi_2(\phi_1^2(\psi - q + r) + 8sp + 4q(q - r + \psi))\Psi_{21} + \phi_1(-\phi_2^2(q - r + \psi) + 8sp - 4q(\psi - q + r))\Phi_{12}) \quad [A\cdot6]$$

$$A_c = D_{ox}\phi_2((2ps - (q - r)(\psi - q + r))\phi_1^2 + 4ps(\psi + q + r))\Psi_{21} + D_{ox}\phi_1((2ps + (q - r)(q - r + \psi))\phi_2^2 - 4ps(\psi - q - r))\Phi_{12} \quad [A\cdot7]$$

$$B_N = 4\psi\sqrt{(q + r)^2 - \psi^2}((q - r + \psi)\Phi_{121} + (r - q + \psi)\Psi_{211}) \quad [A\cdot8]$$

with

$$\Phi_{12} = \left(\cosh\left(\frac{\phi_1}{2}\right) + \sinh\left(\frac{\phi_1}{2}\right)\right)(\cosh\phi_2 + \sinh\phi_2 - 1) \quad [A\cdot9]$$

$$\Psi_{21} = \left(\cosh\left(\frac{\phi_2}{2}\right) + \sinh\left(\frac{\phi_2}{2}\right)\right)(\cosh\phi_1 + \sinh\phi_1 - 1) \quad [A\cdot10]$$

$$\Phi_{121} = \left(\cosh\left(\frac{\phi_1}{2}\right) + \sinh\left(\frac{\phi_1}{2}\right)\right)(\cosh\phi_2 + \sinh\phi_2 + 1) \quad [A\cdot11]$$

$$\Psi_{211} = \left(\cosh\left(\frac{\phi_2}{2}\right) + \sinh\left(\frac{\phi_2}{2}\right)\right)(\cosh\phi_1 + \sinh\phi_1 + 1) \quad [A\cdot12]$$

ORCID

Andrei Kulikovsky https://orcid.org/0000-0003-1319-576X

References

1. A. Lasia, *Electrochemical Impedance Spectroscopy and its Applications* (Springer, New York, NY) (2014).
2. M. E. Orazem and B. Tribollet, *Electrochemical Impedance Spectroscopy* (Wiley, New-York, NY) 2nd ed. (2017).
3. A. M. Dhirde, N. V. Dale, H. Salehfar, M. D. Mann, and T.-H. Han, "Equivalent Electric Circuit Modeling and Performance Analysis of a PEM Fuel Cell Stack Using Impedance Spectroscopy." *IEEE Trans. Energy Conv*, **25**, 778 (2010).
4. J. Kim, J. Lee, and B. H. Cho, "Equivalent Circuit Modeling of PEM Fuel Cell Degradation Combined With a LFRC." *IEEE Trans. Ind. Electronics*, **60**, 5086 (2013).
5. D. Macdonald, "Reflections on the History of Electrochemical Impedance Spectroscopy." *Electrochim. Acta*, **51**, 1376 (2006).
6. T. E. Springer, T. A. Zawodzinski, M. S. Wilson, and S. Gottesfeld, "Characterization of Polymer Electrolyte Fuel Cells Using AC Impedance Spectroscopy." *J. Electrochem. Soc.*, **143**, 587 (1996).
7. M. Eikerling and A. A. Kornyshev, "Electrochemical Impedance of the Cathode Catalyst Layer in Polymer Electrolyte Fuel Cells." *J. Electroanal. Chem.*, **475**, 107 (1999).
8. Z. Tang, Q.-A. Huang, Y.-J. Wang, F. Zhang, W. Li, A. Li, L. Zhang, and J. Zhang, "Recent Progress in the Use of Electrochemical Impedance Spectroscopy for the Measurement, Monitoring, Diagnosis and Optimization of Proton Exchange Membrane Fuel Cell Performance." *J. Power Sources*, **468**, 228361 (2020).
9. J. Huang, Y. Gao, J. Luo, S. Wang, C. Li, S. Chen, and J. Zhang, "Editors' Choice–Review–Impedance Response of Porous Electrodes: Theoretical Framework, Physical Models and Applications." *J. Electrochem. Soc.*, **167**, 166503 (2020).
10. A. A. Kulikovsky, "Exact Low-Current Analytical Solution for Impedance of the Cathode Catalyst Layer in a PEM Fuel Cell." *Electrochim. Acta*, **147**, 773 (2014).
11. A. A. Kulikovsky, "One-Dimensional Impedance of the Cathode Side of a PEM Fuel Cell: Exact Analytical Solution." *J. Electrochem. Soc.*, **162**, F217 (2015).
12. A. Kulikovsky, "Analytical Impedance of Oxygen Transport in the Channel and Gas Diffusion Layer of a PEM Fuel Cell." *J. Electrochem. Soc.*, **168**, 114520 (2021).
13. A. Kulikovsky and O. Shamardina, "A Model for PEM Fuel Cell Impedance: Oxygen Flow in the Channel Triggers Spatial and Frequency Oscillations of the Local Impedance." *J. Electrochem. Soc.*, **162**, F1068 (2015).
14. T. Reshetenko and A. Kulikovsky, "Variation of PEM Fuel Cell Physical Parameters with Current: Impedance Spectroscopy Study." *J. Electrochem. Soc.*, **163**, F1100 (2016).
15. A. Kulikovsky, *Analytical Models for PEM Fuel Cell Impedance* (Self-publishing, Eisma) (2022), https://www.amazon.com/Andrei-Kulikovsky/e/B00KBW7KVY.
16. A. Kulikovsky, "Analytical Impedance of Two-Layer Oxygen Transport Media in a PEM Fuel Cell." *Electrochem. Comm.*, **135**, 107187 (2022).
17. M. Eikerling and A. A. Kulikovsky, *Polymer Electrolyte, Fuel Cells: Physical Principles of Materials and Operation* (CRC Press, London) (2014).
18. A. A. Kulikovsky, "The Regimes of Catalyst Layer Operation in a Fuel Cell." *Electrochim. Acta*, **55**, 6391 (2010).